Supporting Information

Rational Selection of Small Aromatic Molecules to Functionalize Graphene for Enhancing Capacitive Energy Storage

Yi Zhao, Jinzhang Liu, Na Wang, Qi Li, and Mingjun Hu*

School of Materials Science and Engineering, Beihang University, Beijing 100191, China.

*E-mail: ljz78@buaa.edu.cn

1. Experimental Details

Adsorption of Small Aromatic Molecules onto NG Films. The small aromatic molecules selected in this work are insoluble in cold water, but soluble in hot water with adjusted pH value. Typically, water solutions containing ammonia (0.05 wt.%) or dilute sulfuric acid (1 M) were used for dissolving these organic molecules at 60 °C (**Figure S**1a) and at a concentration of 0.06 M. After, the solution was vacuum filtered using a porous membrane with pore size of 0.22 μm to obtain a clear solution for functionalizing NG films. After immersed into the solution at 60 °C for 3 h, the NG film with adsorbed molecules was removed and stored in DI water. It should be noted that some solutions undergo color change with ageing (**Figure S**1b). The B solution changed from clear to light yellowish after ageing for several days, indicating a good stability of the B molecule. The darkened color of A and C solution can be attributed to the oxidation of –OH groups.

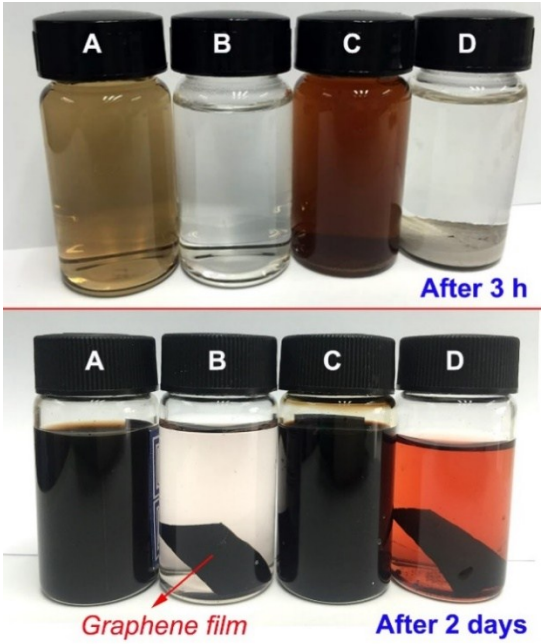

Figure S1. Aqueous solutions of four different aromatic molecules. Their solution colors evolved differently with ageing.

Electrochemical Testing. Symmetric cells were fabricated with two identical electrode films and membrane separator in between. Coin cells were made using 316 stainless steel cases and 1 M H_2SO_4 or 2 M Li_2SO_4 (pH~2) aqueous electrolyte. Prior to the device assembly, electrode films and porous membranes were soaked in the electrolyte for 2 h.

Characterization. The morphology of functionalized NG films was studied using a FE-SEM (Zeiss Supra55). AFM images were obtained by on an ICON Veeco/Bruker microscope. For AFM analysis, graphene sheets were dispersed onto mica substrates. XPS spectra of the as obtained samples were conducted on a Thermo Scientific Escalab 250Xi.

2. SEM Observation

Figure S2 shows cross-sectional SEM images of NG films functionliazed by different aromatic molecules. All films consist of rumpled NG sheets, and there is no trace of aggregated organic molecues inside the film. The rumple feature of NG sheets help inhibit the restacking.

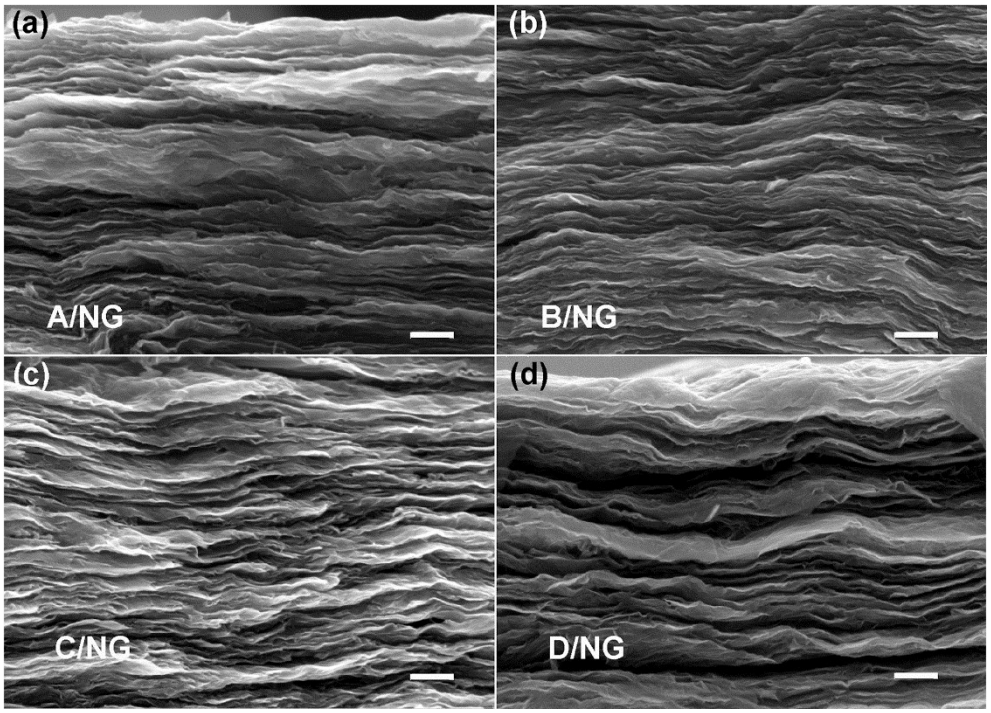

Figure S2. Cross-sectional SEM images of (a) A/NG, (b) B/NG, (c) C/NG, and (d) D/NG films. The scale bar in each image represents 200 nm.

3. FT-IR Analysis

To further confirm the adsorption of organic molecules onto NG sheets, we used Fourier transform infrared spectroscopy (FT-IR) to study the samples. For instance, **Figure S**2 shows three spectra from pure A molecules (4,4′-oxydiphenol), shattered NG, and A/NG (after surface functionalization by A molecules). Apparently, the two peaks assigned to C−H and C−O bonds of A molecules are discernible in the IR spectrum of A/NG, as marked by two green circles. Tough signals are weak due to the monolayer of A molecules over graphene surface, it confirms the adsorption of organic molecules onto graphene.

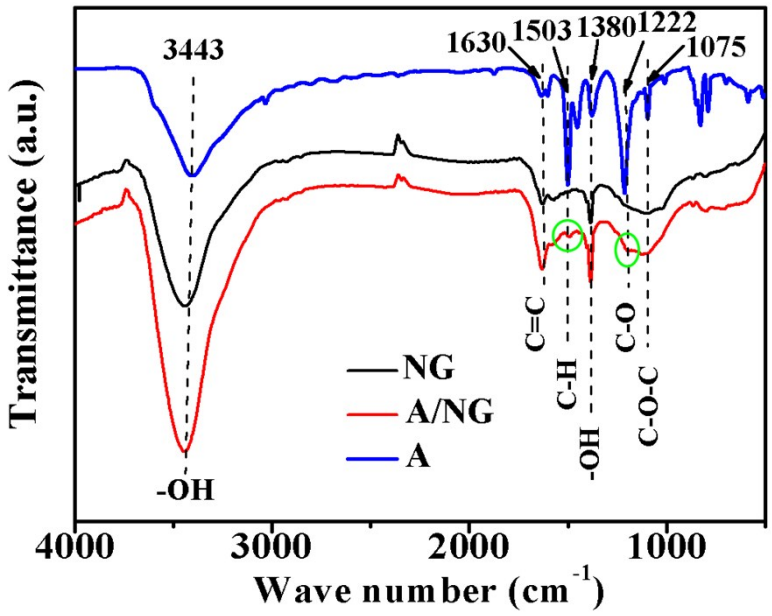

Figure S3. FT-IR analysis of pure A molecules, NG sheets, and NG sheets functionalized by A molecules (A/NG).

4. Capacitance calculation

The gravimetric specific capacitances (C_g) was calculated using galvanostatic CD curves, according to the following equations:

$$C_g = (I\Delta t)/(\Delta V) \quad (1)$$

where I is the current density (A g^{-1}), Δt is the time for a full discharge, and ΔV is the potential window. Using CV loops, the specific capacitance C_g of one electrode can be calculated according to:

$$C_g = \oint IdV/(mv\Delta V) \quad (2)$$

Here, I is the current, $\oint IdV$ is the area of a CV loop, m is the mass of one electrode, v is the potential scan rate, and ΔV is the voltage window. The energy density E (in Wh kg^{-1}) was estimated by using Eq.(3):

$$E = C_g V^2/(8 \times 3.6) \quad (3)$$

5. Calculation for the energy change in a redox process involving amino or hydroxyl groups

Bond energy values used for calculation are as following:

C–O 358; O–H 463; C=O 799; C-N 293; N-H 391; C=N 615 (kJ mol^{-1})

For the -OH group linked to a carbon ring, according to Eq. (4), the release of H, caused the change of enthalpy: 358+463-799 = 22 (kJ mol^{-1}).

$$C–OH \rightarrow C=O \qquad (4)$$

Similarly, according to Eq.(5), the release of a hydrogen atom from an amino group causes the energy change as: 293+2×391-(615+391) = 69 (kJ mol^{-1}).

$$C\text{-}NH_2 \rightarrow C=NH \qquad (5)$$

Therefore, the redox process at amino group requires more energy than that of hydroxyl group, which accounts for the robustness of aromatic molecules containing amino groups, such as the B molecule that exhibits more stable pseudocapacitive performance and better cycling performance compared to those counterparts containing hydroxyl groups.

6. Impedance Spectra

Figure S5 shows impedance spectra of symmetric cells using five different electrodes in H_2SO_4 electrolyte, respectively. In the inset, at low frequency, the B/NG device shows the largest phase change up to -84.4^o, whereas the A/NG devices shows the lowest phase change at -76.5^o.

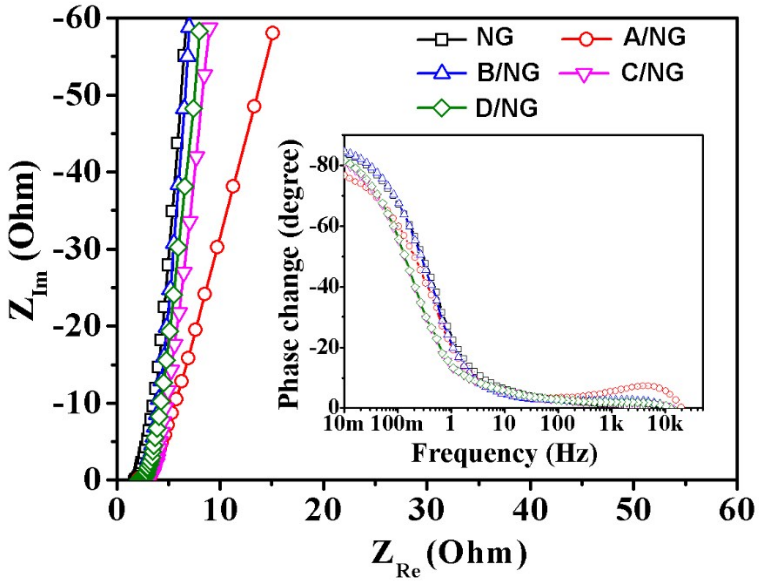

Figure S4. Impedance spectra from five symmetric cells using different electrodes. The inset shows the phase change against sweeping frequency for each device.

7. Testing Symmetric Cells Based on A/NG films within Different Potential Windows

Sets of CV and CD curves were collected by appliying different potential windows. In **Figure S3**a, after 1.4 V, the right corner of CV loops keeps riging with increasing the voltge, and the polarization of electrolyte is obvious at higher voltage. In **Figure S3**b, apparently the voltage of 1.7 V is too high to deliver charges into the electrode film.

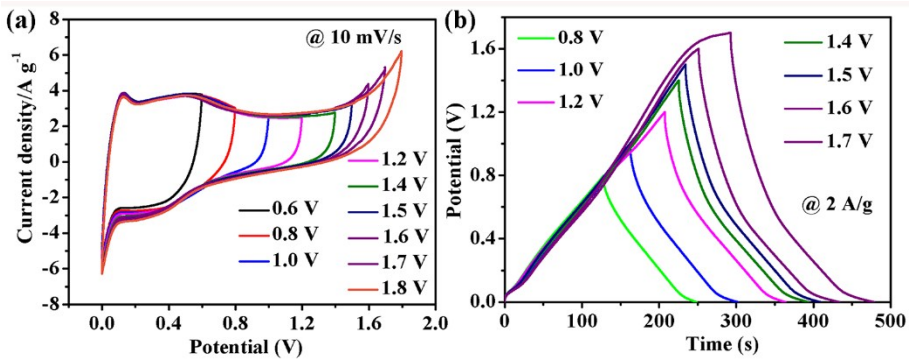

Figure S5. (a) CV and (b) CD curves of the symmetric cell based on A/NG films in

Li_2SO_4 aqueous electrolyte within different potential windows.

8. Specific Capacitance of B/NG Films Calculated from GCD Curves

Figure S4 shows the dependence of specific capacitance of B/NG film against the discharging current, calculated from GCD curves. The use of Li_2SO_4 aqueous electrolyte extends the operating voltage window to 1.6 V, though the correesponding specific capacitance is a bit lower compared to that in H_2SO_4 electroyte.

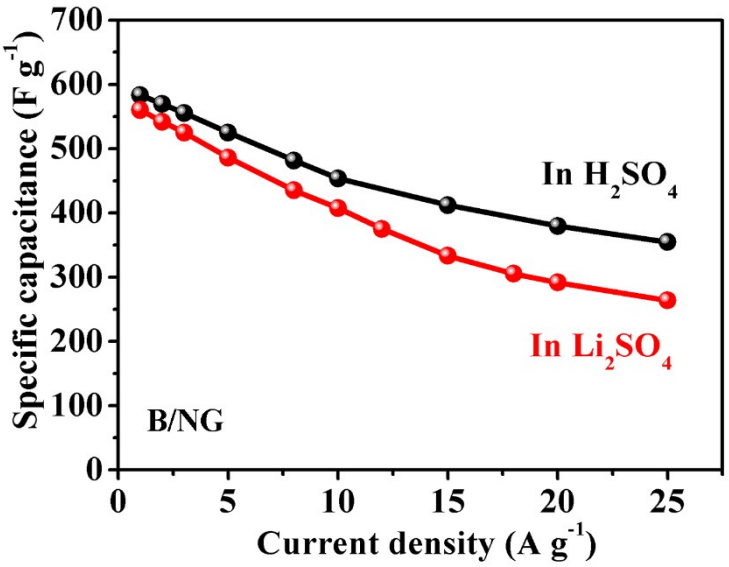

Figure S6. Specific capacitance of B/NG films in different electrolyte versus current density used in GCD measurement.

9. The Cyclic Stability of Funcrtionalized NG Film Electrodes in Different Electrolytes

The shape variation of CV loops after different cyling numbers can help understand the change of capacitance, i.e., from the loop area, and the vriation of redox behavior. **Figures S4**a **S4**b, and **S4**c show CV loops at 10 mV s^{-1} after different cycle numbers,

collected from symmetric cells based on A/NG, B/NG, and C/NG films, respectively. In **Figure S4**a, at the initial stage the CV loop had no redox peaks in the voltage range of 0–0.2 V. However, with cycling the charge-discharge process, sharp redox peaks started to emerge after tens of cycles and remianed stable. Presumably, –OH groups at one side of a molecule from two different molecues combined to release H_2O and to form –O– bonds that are responsible for this redox peak. In terestingly, when in Li_2SO_4 aqueous electrolyte, the sharp redox peak at low voltage emerged in the initial stage, but vanished with cycling the device, as shwon in **Figure S**4d. Therefore, for A molecules the electrochemical redox of –OH groups by H^+ is different from that by Li^+. For the B molecules that contain only $–NH_2$ groups, in H_2SO_4 electrolyte the potential position of their redox peaks keeps shifting from high to low with cycling (**Figure S4**b). However, when in Li_2SO_4 electrolyte the redox peak position is almost static even after 5,000 cycles. Also, for C molecules the redox voltage of active groups in Li_2SO_4 is more stable than in Li_2SO_4. We conclude that these redox groups undergo transformation when repeatedly reacting with H^+, whereas the status of $–NLi_2$ or –OLi groups is rather stable against cyling test.

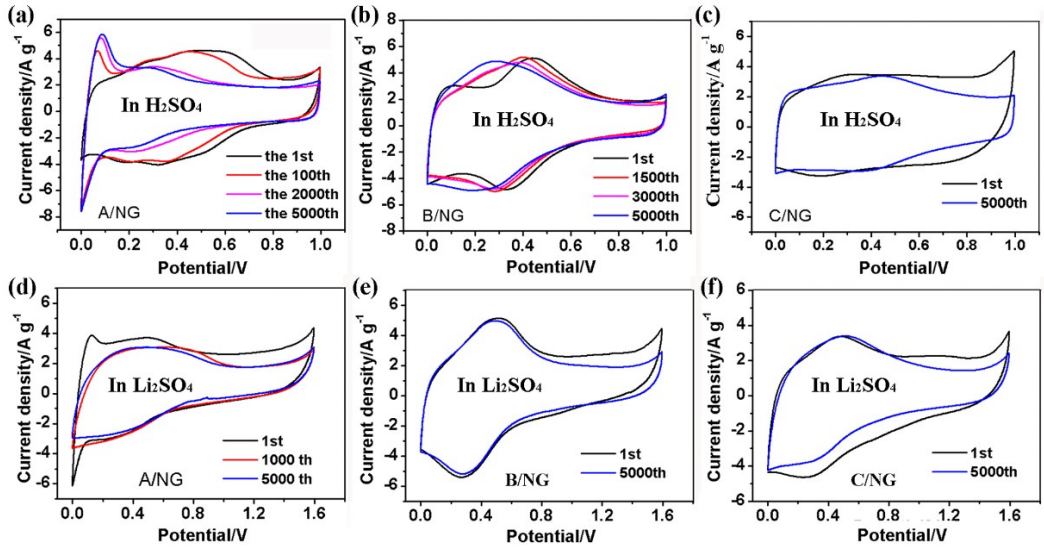

Figure S7. (a, b, and c) CV loops at 10 mV s^{-1} from symmetric cells based on A/NG,

B/NG, and C/NG films, recorded at different cycle numbers, respectively. (d, e, and f). Within a wider voltage window of 1.6 V and using Li_2SO_4 electrolyte, CV loops at 10 mV s^{-1} were collected after different cycling durations for A/NG, B/NG, and C/NG films, respectively.

10. Comparison of Cycling Stability

The three cells based on A/NG, B/NG, and C/NG films, respectively, were tested by running CD cycles at 10 A g^{-1}. Their cycling stabilities with using H_2SO_4 and Li_2SO_4 aqueous electrolytes are compared in **Figure S6**a and **S6**b, respectively. The sequence of stability for the three types of molecules is $B > C > A$.

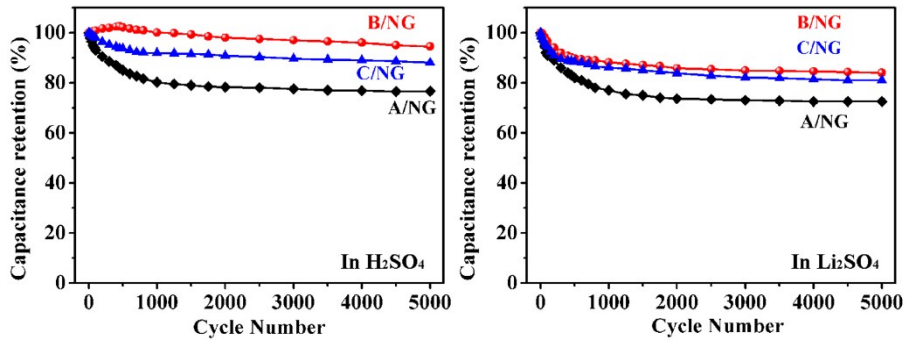

Figure S8. Comparison of capacitance retention for three cells based on A/NG, B/NG, and C/NG films in two different aqueous electrolytes: (a) H_2SO_4 and (b) Li_2SO_4. Applied potential windows for the two electrolytes were 1.0 V and 1.6 V, respectively.

11. Electrochemical Measurement on NG Films Functionalized by Molecules of Pyromellitic Acid

In this paper we selected aromatic molecules containing -NH_2 of -OH, or both, to functionalize NG films for adding pseudocapacitance. In fact, we also used other organic molecules for comparison, and some of them have no any effect on enhancing

the capacitance. For instance, pyromellitic acid was used to functionalize the NG film, of which the weight was 16% increased due to adsorption of molecules. NG films befor and after surface functionalization were electrochemically tested using a two-electrode configuration and H_2SO_4 electrolyte. As shown in **Figure S4**a, the area of CV loop corresponding functionalized NG film shows no much change compared to that of NG film. Also, the time span of GCD curve is a bit decreased after the adsorption of pyromellitic acid (**Figure S4**b). The inset of Figure S4b shows the molecular structure of pyromellitic acid. Our results indicate that the pyromellitic acid molecules over NG surface have no contribution to pseudocapacitance.

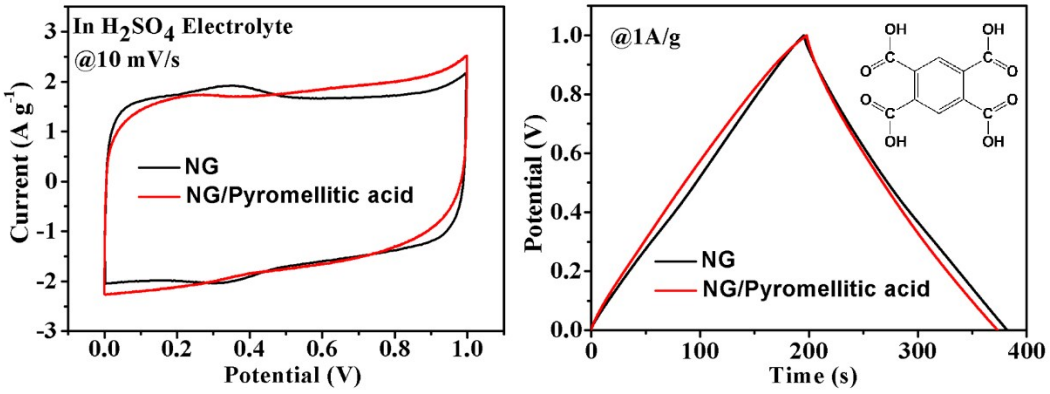

Figure S9. (a) CV and (b) GCD curves of symmetric cells using NG and pyromellitic-acid-functionalized NG films as electrodes, respectively, showing no added pseudocapacitance after adsorption of this type of molecules. The inset in (b) shows the molecular structure of pyromellitic acid.

12. Lightening Tri-Color LEDs

Four button cells using B/NG films as electrodes and Li_2SO_4 aqueous electrolyte were connected in series to demonstrate their capability of powering 8 LEDs. The areal mass loading of B/NG film is 1.5 mg cm^{-2}. The charging voltage is up to 6 V, and these LEDs

were lit up for 5 min. The tri-color LED can alternatively emit blue, green and red lights at a static driving voltage. However, normally the short the light wavelength, the higher the threshold of driving voltage. Hence, with the decay of output voltage from supercapacitors, finally only red light kept glowing.

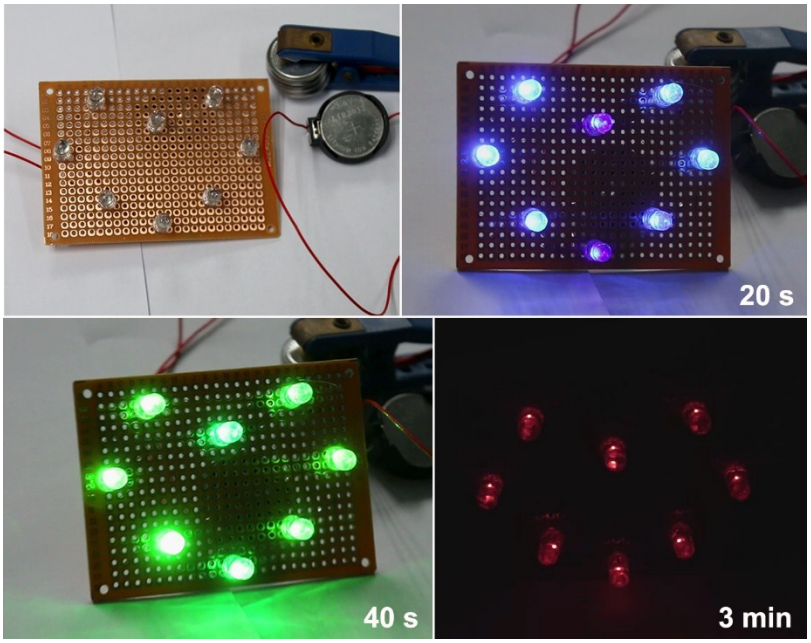

Figure S10. Six tri-color LEDs lit by four button cells after different durations. The cell contains B/NG films as electrodes and Li_2SO_4 aqueous electrolyte.